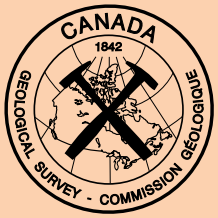


Geological Survey of Canada

CURRENT RESEARCH
2007-B1

# Remote predictive mapping of surficial materials on northern Baffin Island: developing and testing techniques using Landsat TM and digital elevation data

*O. Brown, J.R. Harris, D. Utting, and E.C. Little*

**2007**

CURRENT RESEARCH

Natural Resources Canada Ressources naturelles Canada

Canada

ISSN 1701-4387
Catalogue No. M44-2007/B1E-PDF
ISBN 978-0-662-44951-5

A copy of this publication is also available for reference in depository libraries across Canada through access to the Depository Services Program's Web site at http://dsp-psd.pwgsc.gc.ca

A free digital download of this publication is available from GeoPub: http://geopub.nrcan.gc.ca/index_e.php

Toll-free (Canada and U.S.A.): 1-888-252-4301

***Critical reviewers***
*Danny Wright*
*Donald James*

***Authors***

***Olivia Brown***
***Daniel Utting***
***(dutting@nrcan.gc.ca)***
*Canada-Nunavut Geoscience Office*
*626 Tumiit Plaza, Suite 202*
*Iqaluit, Nunavut X0A 0H0*

***Edward C. Little***
***(elittle@nrcan.gc.ca)***
*Geological Survey of Canada,*
*3303-33rd St., N.W.*
*Calgary, Alberta T2L 2A7*

***Jeff Harris***
***(harris@nrcan.gc.ca)***
*Geological Survey of Canada,*
*601 Booth Street*
*Ottawa, Ontario K1A 0E8*

Publication approved by GSC Central Canada

Correction date:

# Remote predictive mapping of surficial materials on northern Baffin Island: developing and testing techniques using Landsat TM and digital elevation data

O. Brown, J.R. Harris, D. Utting, and E.C. Little

Brown, O., Harris, J.R., Utting, D., and Little, E.C., 2007: Remote predictive mapping of surficial materials on northern Baffin Island: developing and testing techniques using Landsat TM and digital elevation data; Geological Survey of Canada, Current Research 2007-B1, 12 p.

**Abstract:** Considering the vastness of Nunavut, the paucity of regional-scale surficial geology maps for the territory, the significant expense of working in a remote region, and the increasing availability of affordable, remotely sensed data, it is timely to develop and test remote predictive mapping techniques for producing surficial geology maps. The goal of this remote predictive mapping project is to produce a surficial materials map, which will be used to expedite subsequent ground-based mapping and sampling.

This paper describes techniques used to produce a surficial materials map for an area in northern Baffin Island using remote predictive mapping techniques with Landsat TM and digital elevation data. The predictive maps produced in advance of the field work (i.e. "ground truthing") were found to be approximately 50% accurate. To improve remote predictive mapping accuracy to at least 80%, high-resolution imagery may need to be included in the remote predictive mapping protocol.

**Résumé :** Compte tenu de la vaste étendue du Nunavut, de la rareté des cartes d'échelle régionale des dépôts meubles du territoire, des dépenses importantes encourues lors de travaux en région éloignée et de la disponibilité croissante de données de télédétection abordables, il est opportun d'élaborer et de mettre à l'essai des techniques de cartographie prévisionnelle à distance pour la production de cartes des dépôts meubles. Le présent projet de cartographie prévisionnelle à distance avait pour objectif de produire une carte des dépôts meubles qui servira à accélérer les travaux subséquents de cartographie et d'échantillonnage sur le terrain.

Le présent article décrit les techniques utilisées afin de produire une carte des dépôts meubles pour une région dans le nord de l'île de Baffin en utilisant des techniques de cartographie prévisionnelle à distance avec des données du Landsat-TM et des données altimétriques numériques. On estime que les cartes prévisionnelles produites avant les travaux sur le terrain (c.-à-d. avant la vérification au sol) avaient une exactitude de 50 %. Afin d'augmenter à au moins 80 % l'exactitude de la cartographie prévisionnelle à distance, il faudrait éventuellement inclure des images à haute résolution dans le protocole de cartographie prévisionnelle à distance.

## INTRODUCTION

The geoscience knowledge base for Nunavut is generally inadequate to meet the current demands of the mineral exploration industry. Improving the knowledge base requires the collection of large amounts of high-quality geoscience data. Capturing geoscience data using traditional ground-based activities is resource intensive, and regional-scale mapping projects can take years to complete. A map generated by integrating and interpreting various types of remotely sensed data in concert with ground-based field observations and produced in advance of field work, has significant potential for increasing the effectiveness and efficiency of regional-scale geoscience studies.

The primary objective of remote predictive mapping (RPM) for the North Baffin Project is to predict the location of till with 80% accuracy. This involves supervised classification of Landsat TM and digital elevation model (DEM) data based on training areas representative of each surficial unit to be classified followed by maximum likelihood classification to produce predictive (classified) maps.

Landsat TM and DEM data for Nunavut are readily available from Natural Resources Canada; in fact Landsat data is free from the Geogratis Web site (http://geogratis.cgdi.gc.ca/). The North Baffin Project area (NTS 37 E and 37 H/south, Fig. 1) provides suitable conditions to predict surficial geology using remotely sensed data as the vegetation cover is minimal.

This report provides a summary of the methodology used to create the predictive surficial geology maps, an assessment of the accuracy of the predictive maps from a comparison with the original training sites and field data, and recommendations for futures studies

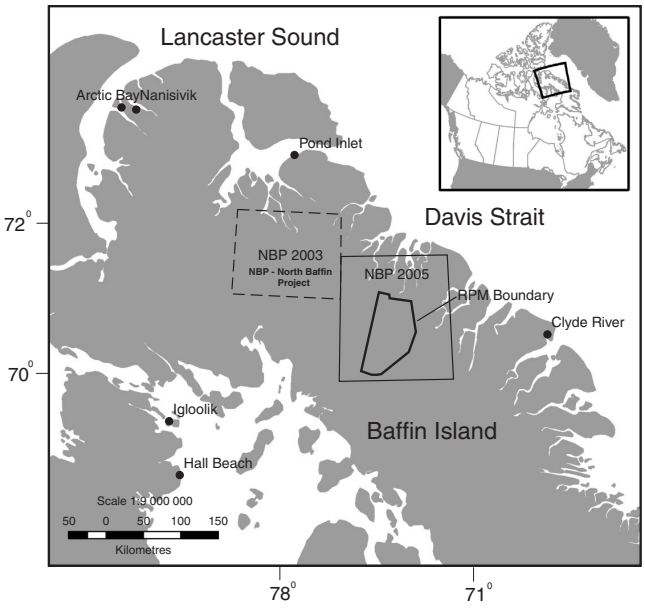


**Figure1**. Location of the North Baffin and remote predictive mapping projects.

## STUDY AREA

The study area is on northeastern Baffin Island in NTS 37 E (Conn Lake sheet; Fig. 1) and lies mainly within the Baffin Uplands, north of the Barnes Ice Cap (Bostock, 1970). It is underlain by rocks of the Rae domain western Churchill Province, an Archean granite-greenstone terrane including north- to northeast-striking rocks of the Mary River group (Jackson, 2000). Mapping of the surficial geology at 1:500 000 scale was completed for a portion of the study area by Hodgson and Haselton (1974). The most recent mapping was undertaken by Utting et al. (2006). The study area contains relatively little vegetation cover. Grasses are restricted mainly to river valleys and lichen covers some areas. Lichen-free areas are associated with the expansion of perennial snowfields during the Little Ice Age (Wolken et al., 2005).

Geomorphological features in the study areas include steep-sided fiords, high plateaus, rolling hills, valleys, moraines, flutings, deltas, meltwater channels, and eskers (Little et al., 2004). The study area is dominated by glacial drift; however, bedrock, glaciolacustrine, and fluvial material also occur sporadically throughout the study area.

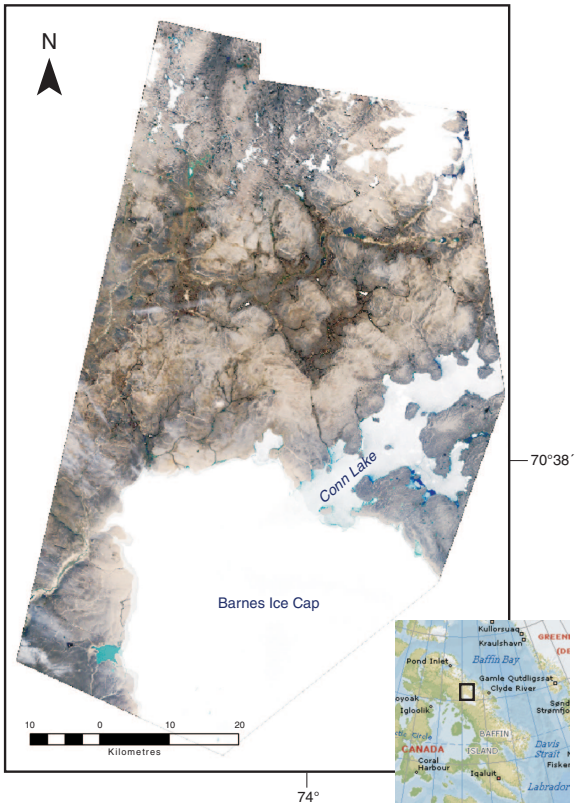


**Figure 2.** LANDSAT TM 30 m resolution data of the study area shown as a 3, 2, 1 (RGB) natural colour composite

## DATA AND PREPROCESSING

Landsat TM and DEM data were used to create the remote predictive maps. The Landsat TM data, acquired August 2, 2002 (Fig. 2), has a spatial resolution of 30 m. Landsat TM bands 1 (0.45–0.52 µm), 2 (0.52–0.60 µm), 3 (0.63–0.69 µm), 4 (0.76–0.90 µm), 5 (1.56–1.75 µm), and 7 (2.08–2.35 µm) were used in the analysis. The digital elevation model (Fig. 3), built from National Topographic Data Base contour lines, has a resolution of 250 m.

Areas of ice, water, snow, and cloud were removed from the Landsat data using band thresholding techniques based on ratio images of various Landsat bands (see Harris et al., 1998) before performing classification.

## METHODS

Maximum likelihood classification was used to create the predictive surficial geology maps. Maximum likelihood classification, an algorithm common to most remote sensing software packages, groups pixels of statistically similar reflectance from a remotely sensed data set into classes on the basis of signatures derived from training areas, which, in this study, represent classes of surficial materials. Maximum likelihood classification was used successfully by Rencz et al. (2000) to map bedrock units in the Borden Peninsula in Northern Baffin Island.

Training areas for each of the surficial units to be classified were identified through airphoto interpretation. The first set of training areas contained three classes, i.e. 'till', which includes glacial till deposits, 'fluvial', which includes fluvial deposits of finer grained sediments that appear bright (i.e. highly reflective) on the Landsat imagery, and 'other', which includes all other surficial material. Figure 4 shows field photographs of the various surficial units. Many training areas were visited in the field to assess their character and quality.

Spectral signatures characterizing each training area (surficial unit) were then gathered from the six Landsat bands and the DEM. The statistical separability of the training classes was evaluated using a transformed divergence (TD) measure (Richards and Jia, 2006). Preliminary statistical analysis indicated that the 'other' class was not statistically separable from the 'till' class; therefore, the 'other' class was further divided into two classes, 'glaciolacustrine' and 'bedrock', by assessing airphotos and Landsat imagery (Fig. 2). The new set of training areas was evaluated and the statistical separability of the classes was improved for both the Landsat and DEM data.

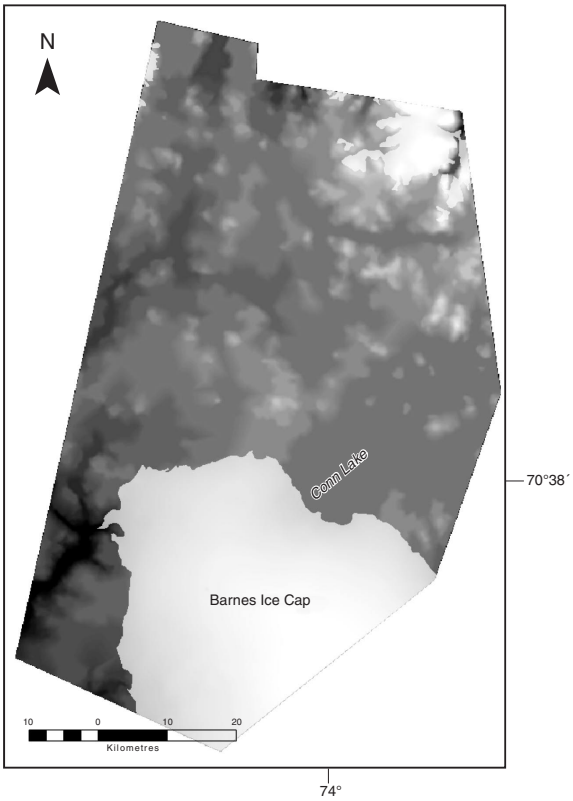


**Figure 3.** Digital elevation model of the study area with 250 m resolution created from National Topographic Data Base contour lines. White to dark tones reflect high to low elevations.

The training areas were divided into two groups (A and B) to test for spectral variability within the training sites. Classified maps were first generated using each training group from Landsat data and subsequently from the combined Landsat and DEM data set, as this allowed for evaluating whether incorporating elevation data improved classification accuracies. The classified maps were spatially filtered using different-sized median and majority filters to improve the spatial integrity of the maps and remove isolated pixels or small groups of pixels. The resulting filtered and unfiltered maps derived from group A training areas were then compared with the map derived from group B training areas. Classification was then performed on the Landsat data and on the combined Landsat and DEM data set using all training areas. The unfiltered and filtered classification maps were then compared with each group of training areas and with point data collected in the field to determine which combinations of data, training areas, and filtering offered the best classification results.

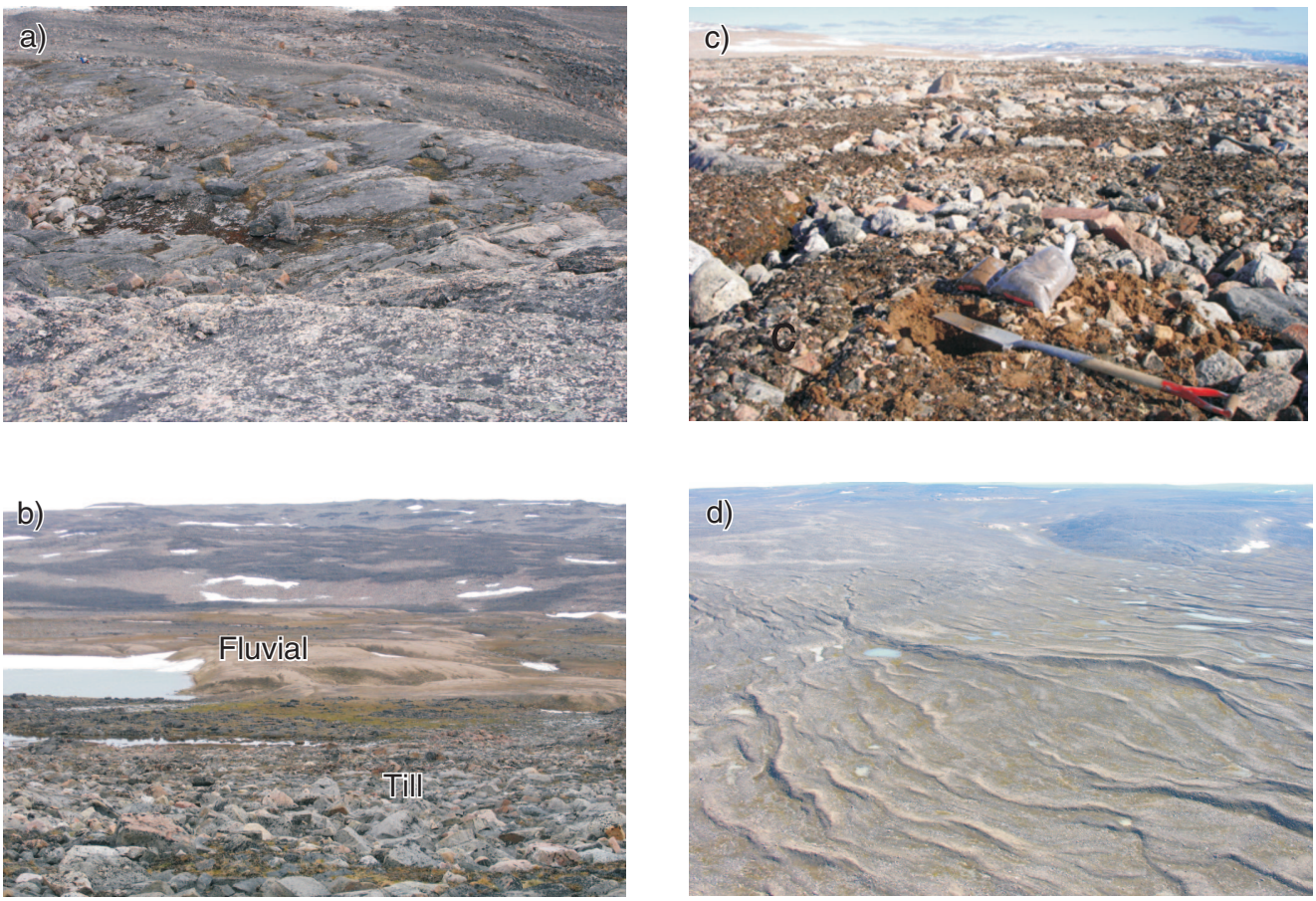


**Figure 4.** Typical training areas: **a)** bedrock; **b)** fluvial material; **c)** till; **d)** glaciolacustrine material.

# RESULTS

## Training site separability

Training classes must be statistically separable to produce accurate classification results (Jensen, 1995; Lillesand et al., 2004). Transformed divergence is a measure of separability between a pair of spectral signatures derived from the Landsat data (all bands) and/or topographic signature (elevation) derived from the DEM; values less than 1 indicate poor separability, those between 1.0 and 1.9, moderate separability with some degree of overlap, and those greater than 1.9, good statistical separability between classes (Ranson et al., 2003; Richards and Jia, 2006).

The first set of training areas included three classes, 'till', 'fluvial', and 'other'. Separability between the 'fluvial' class and the 'till' and 'other' classes meets the ideal TD value of 1.9 (Table 1). Separability between the 'fluvial' and 'till' classes is adequate because finer grained fluvial sediments appear bright on the Landsat imagery. However, the TD value of 0.852 between the 'till' and 'other' classes indicates poor

**Table 1.** Transformed divergence values for three class training sites using Landsat TM data only.

| | Fluvial | Till |
|---|---|---|
| Till | 1.933 | |
| Other | 1.943 | 0.852 |

**Table 2.** Transformed divergence values for three class trainings sites using Landsat TM data and a DEM.

| | **Fluvial** | **Till** |
|---|---|---|
| Till | 1.991 | |
| Other | 1.999 | 1.021 |

separability (Table 1; Fig. 5 and 6). With respect to the Landsat data, the longer wavelength bands (TM 4 and 5) offer better separation between the 'till' and 'other' classes than the shorter wavelength bands (TM 1; Fig. 6).The addition of the DEM in conjunction with Landsat TM data slightly improved separability between the training classes (Table 2), indicating that relief plays a role in controlling the deposition of surficial materials, as might be expected.

The TD value between the 'till' and 'other' classes increased by 19.84% when the DEM data were incorporated, although the two classes are spectrally and topographically similar. Further analysis showed that the low separability values between the 'till' and 'other' classes occurred because of spectral variability within the 'other' class (Fig. 5 and 6). To reduce variability within the 'other' class and to increase separability between the 'till' and 'other' classes, the 'other'

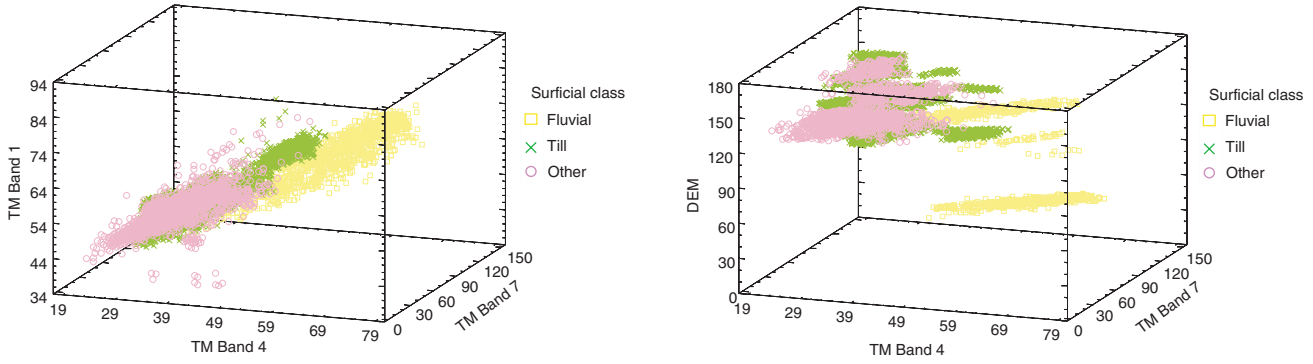


**Figure 5**. Three-dimensional scatter plots showing separability and overlap of the 'fluvial', 'till', and 'other' training sites. Values represent Landsat reflectance and DEM elevation.

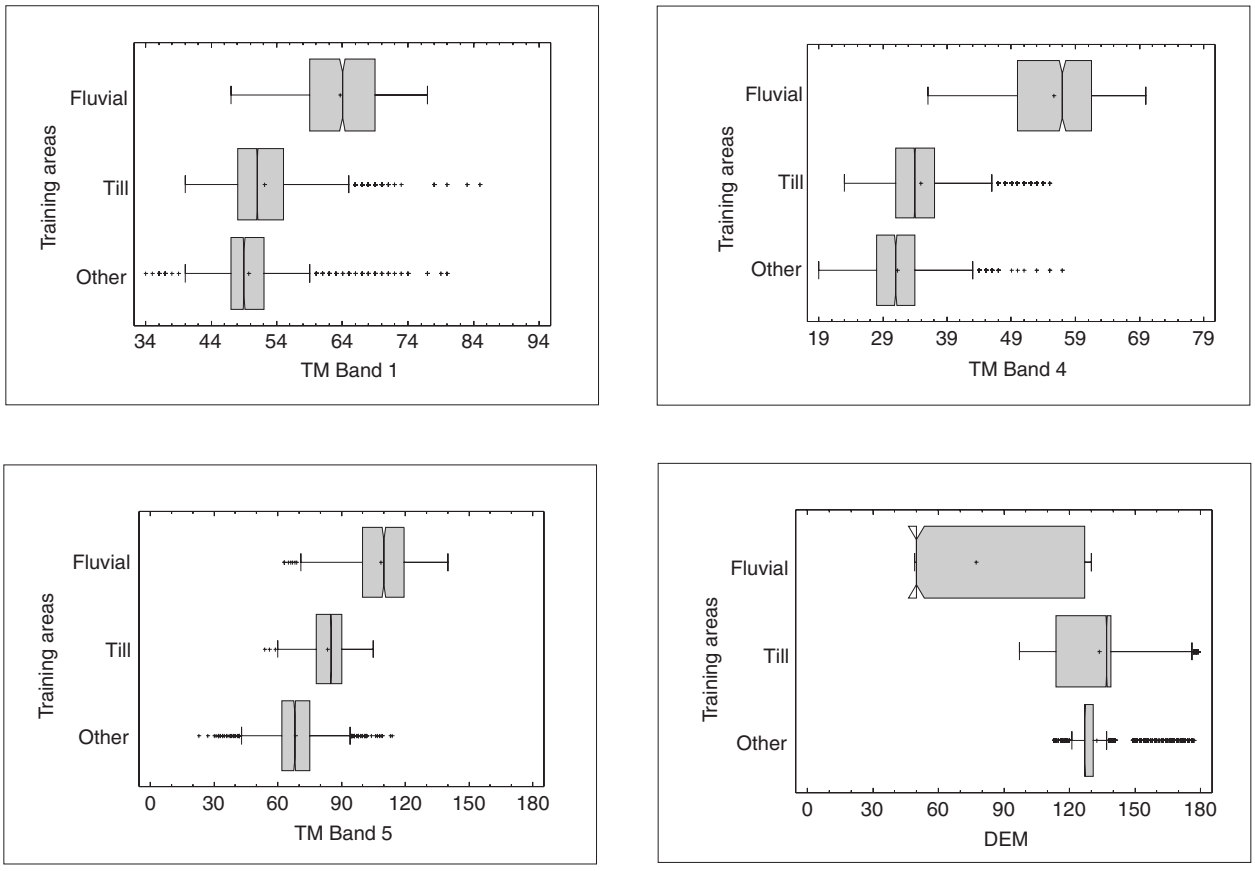


**Figure 6.** Box-and-whisker plots showing separability and overlap of 'fluvial', 'till', and 'other' training site spectra. Values represent Landsat reflectance and DEM elevation.

**Table 3.** Transformed divergence values for four training classes using Landsat TM data only.

| Name | Fluvial | Bedrock | Glaciolacustrine |
|---|---|---|---|
| Bedrock | 1.974 | | |
| Glaciolacustrine | 2.000 | 2.000 | |
| Till | 1.985 | 0.833 | 2.000 |

**Table 4.** Transformed divergence values for four training classes using Landsat TM and DEM data.

| Name | Fluvial | Bedrock | Glaciolacustrine |
|---|---|---|---|
| Bedrock | 2.000 | | |
| Glaciolacustrine | 2.000 | 2.000 | |
| Till | 1.995 | 1.082 | 2.000 |

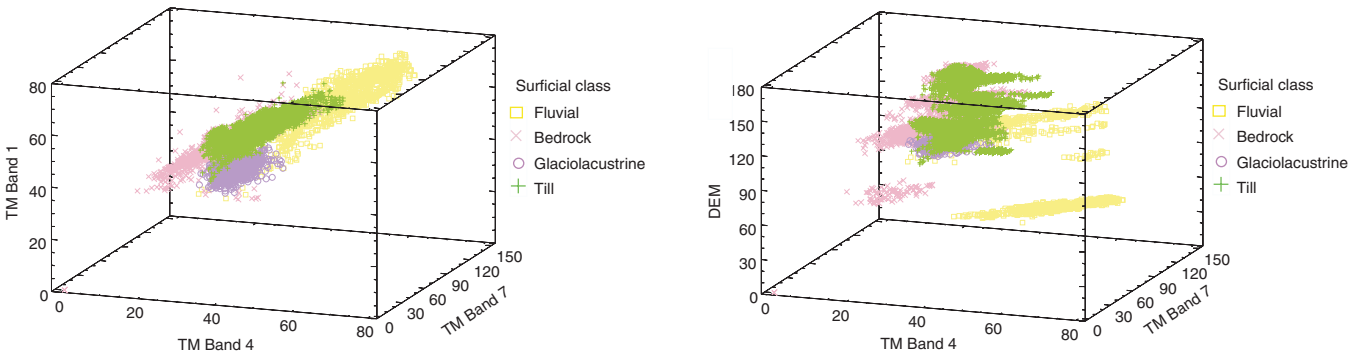


**Figure 7.** Three-dimensional scatter plots showing separability and overlap of the 'fluvial', 'till', 'glaciolacustrine', and 'bedrock' training site spectra. Values represent LANDSAT reflectance and DEM elevation.

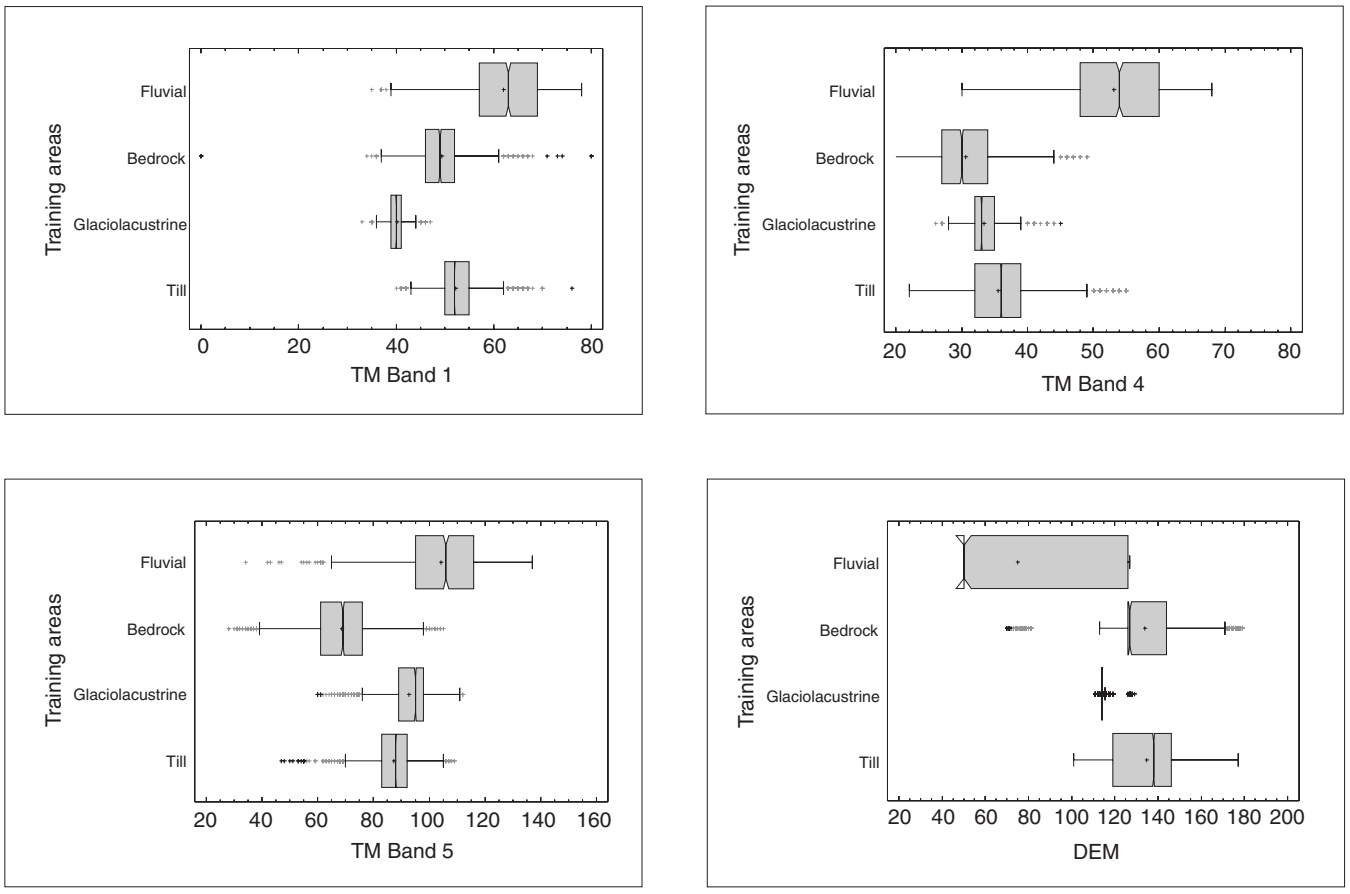


**Figure 8.** Box-and-whisker plots showing separability and overlap of 'fluvial', 'till', 'glaciolacustrine', and 'bedrock' training site spectra. Values represent LANDSAT reflectance and DEM elevation.

class was subdivided into two training classes, 'bedrock' and 'glaciolacustrine', as these are the most significant units within the 'other' class. Tables 3 and 4 show the TD values for the training areas and Figures 7 and 8 show scatter and box-and-whisker plots for the training areas.

Glaciolacustrine areas are separable from the 'bedrock' class as indicated by the high TD values (Tables 3 and 4), with and without inclusion of the DEM. However, the separation between till and bedrock is poor (Fig. 7 and 8). The DEM improved separability between the 'till' and 'bedrock' classes by 29.89%, increasing the TD value from 0.833 to 1.082 (Tables 3 and 4), although these two classes are at best only moderately separable.

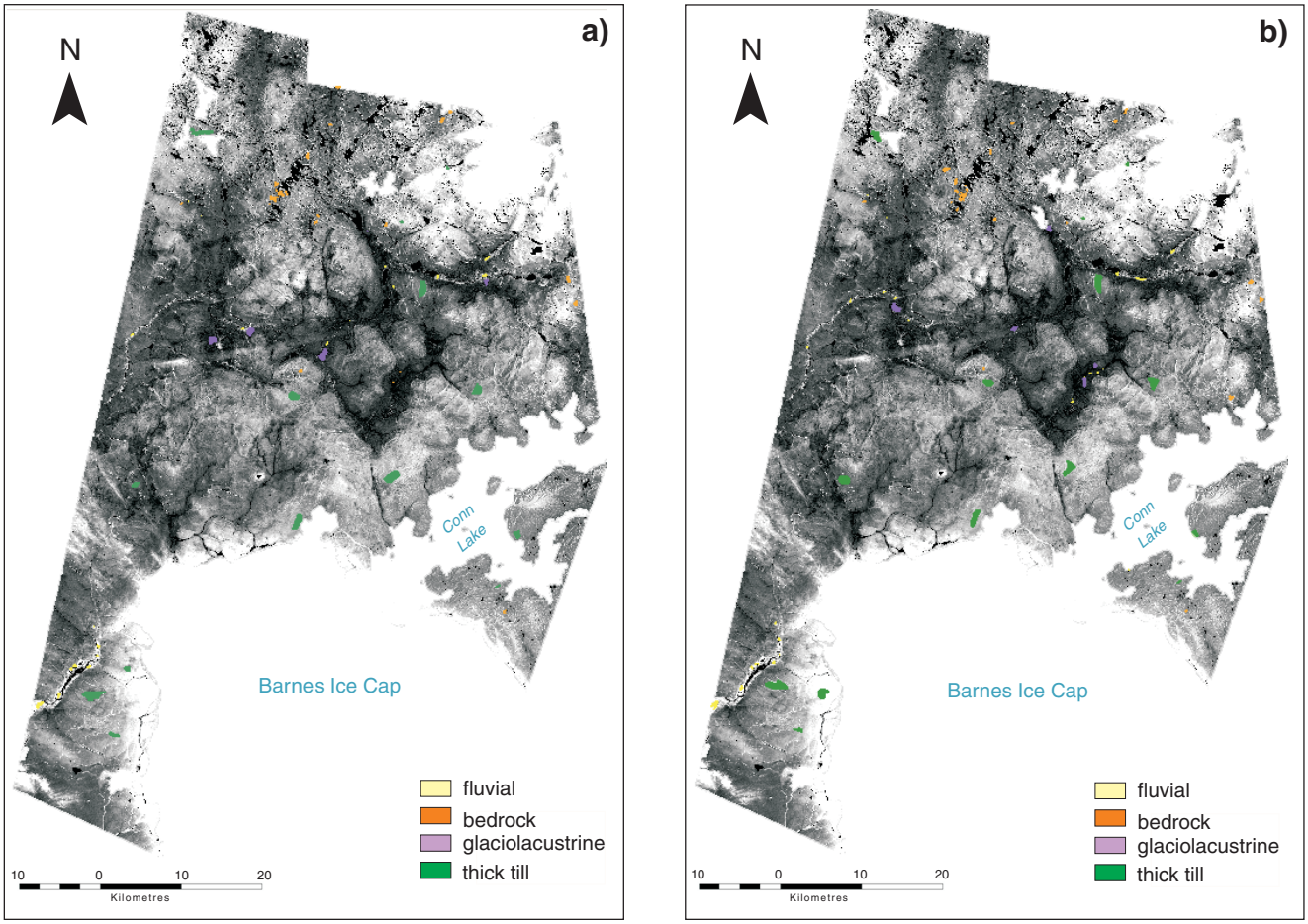


**Figure 9.** Training areas overlaid on a Landsat image (band 4): **a)** group A; **b)** group B.

**Table 5.** Transformed divergence values for group A training sites on Landsat TM data set.

| Name | Fluvial | Bedrock | Glaciolacustrine |
|---|---|---|---|
| Bedrock | 1.902 | | |
| Glaciolacustrine | 2.000 | 2.000 | |
| Till | 1.938 | 1.208 | 1.999 |

**Table 6.** Transformed divergence values for group A training sites on Landsat TM and DEM data sets.

| Name | Fluvial | Bedrock | Glaciolacustrine |
|---|---|---|---|
| Bedrock | 2.000 | | |
| Glaciolacustrine | 2.000 | 2.000 | |
| Till | 1.995 | 1.400 | 2.000 |

**Table 7.** Transformed divergence values for group B training sites on Landsat TM data set.

| Name | Fluvial | Bedrock | Glaciolacustrine |
|---|---|---|---|
| Bedrock | 1.995 | | |
| Glaciolacustrine | 2.000 | 2.000 | |
| Till | 1.998 | 0.759 | 2.000 |

**Table 8.** Transformed divergence values for group B training sites on Landsat TM and DEM data sets.

| Name | Fluvial | Bedrock | Glaciolacustrine |
|---|---|---|---|
| Bedrock | 2.000 | | |
| Glaciolacustrine | 2.000 | 2.000 | |
| Till | 2.000 | 1.013 | 2.000 |

## Variability in training areas

The four-class ('till', 'fluvial', 'bedrock', and 'glaciolacustrine') training area group was divided into two groups (A and B) by splitting larger training areas and distributing smaller training areas between the two groups so they were evenly distributed across the study area (Fig. 9). Transformed divergence values were calculated for group A and group B training sites on both data sets (Tables 5 to 8).

The TD values for each group of training areas indicate that all classes are spectrally distinct except for bedrock and till, as noted above (Fig. 7 and 8; Tables 3 and 4). The inclusion of the DEM has resulted in better separation between till and bedrock, although the two units overlap spectrally. This overlap is expected as boundaries between outcrop and thin till can be transitional in nature. A certain amount of variability exists in the training areas with group A training areas offering better spectral separation between bedrock and till and almost identical separation between the remaining combinations of units (bedrock-fluvial, glaciolacustrine-fluvial, till-fluvial). Maximum likelihood classification was run separately with group A and group B training areas using the Landsat TM and DEM data sets, producing two predictive maps (Fig. 10).

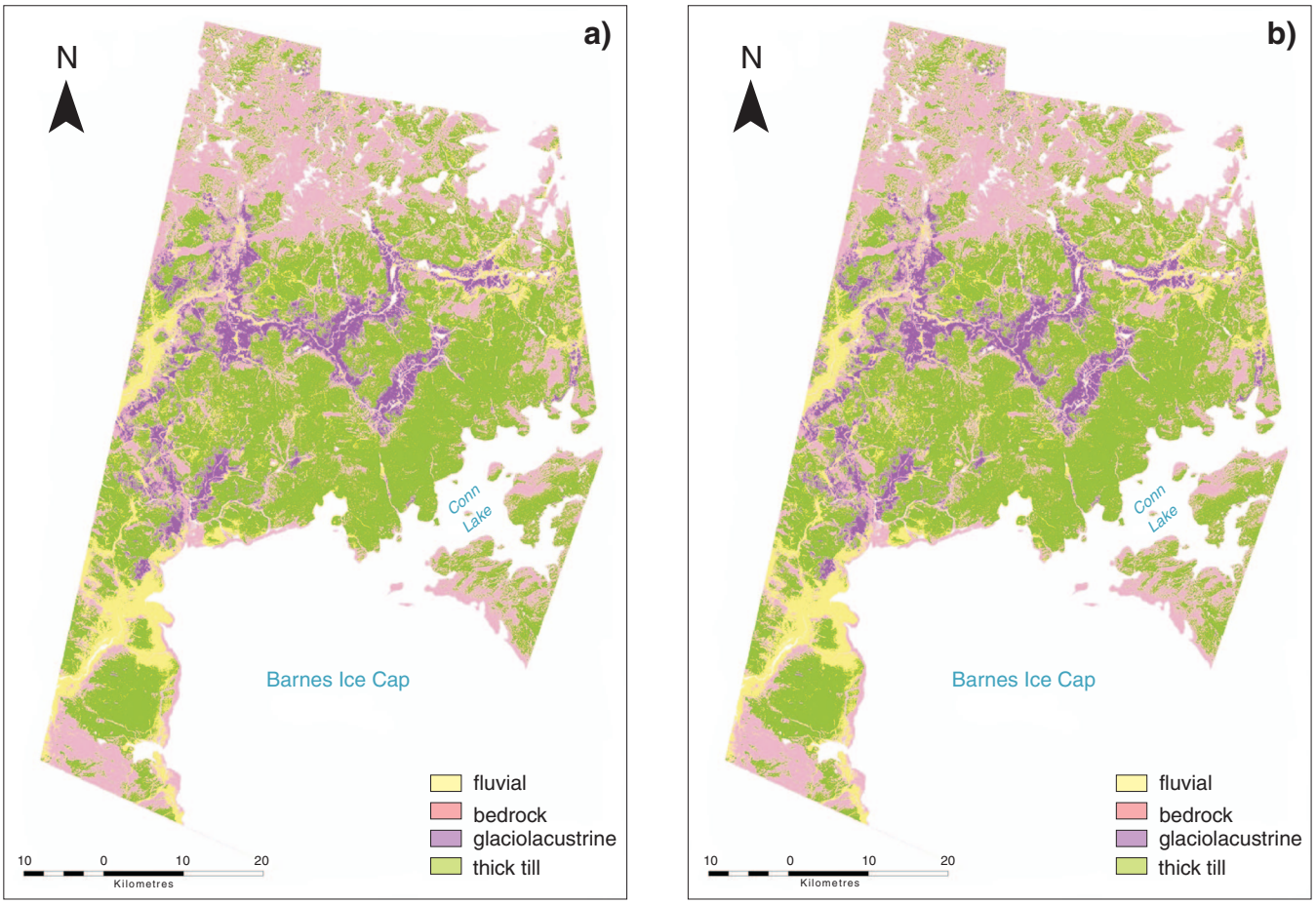


**Figure 10.** Classified map based on **a)** group A training areas and **b)** group B training areas applied to Landsat and DEM data.

**Table 9.** Confusion matrix between maps shown in Figure 10. The numbers represent agreement (%) between classes. Overall agreement between maps

| | | Prediction map derived from Group B training sites | | | |
|---|---|---|---|---|---|
| | | Fluvial | Bedrock | Glaciolacustrine | Till |
| **Prediction map derived from Group A training sites** | Fluvial | 79.01 | 1.69 | 18.43 | 2.97 |
| | Bedrock | 5.46 | 77.96 | 0.76 | 11.87 |
| | Glaciolacustrine | 11.01 | 0.32 | 75.78 | 1.36 |
| | Till | 4.52 | 20.03 | 5.04 | 83.81 |

The resulting classification maps (Fig. 10) were cross-correlated and the overall similarity between the maps was approximately 81% (Table 9). The kappa coefficient (Cohen, 1960), which is a measure for quantifying the level of agreement between two maps with an equal number of classes (ranging from -1.0 for complete disagreement to +1.0 for complete agreement), is 0.69 for these two maps, indicating that they are similar. The greatest difference between the maps (indicated by higher numbers in Table 9 — numbers reflect per cent agreement between classes) is between 'fluvial' and 'glaciolacustrine' classes and 'bedrock' and 'till' classes. For example, with reference to Table 9, the agreement between maps is 79% for the 'fluvial' class and 77.9% for bedrock. However, 18.4% of the pixels classified as fluvial on the prediction map on the basis of training group A were mapped as glaciolacustrine on the prediction map produced from the group B training sites. The confusion for the classification of bedrock was 20% (Table 9). This indicates that notable variation exists between the training areas for groups A and B.

## Classification map results compared with training areas

Filtering the classification maps using a 7 by 7 pixel, median or majority filter improved the classification results by up to 7.5%, when compared with the training areas (Tables 10 and 11).

The *producer's accuracy* is a measure of how well pixels within a training area are classified (Lillesand et al., 2004). The producer's accuracy was consistently highest in the 'fluvial' and 'glaciolacustrine' classes for the predictive (classified) maps. This is to be expected because these classes were the most statistically separable. The best *user's accuracy*, a measure of the probability that a classified pixel actually represents the proper class on the ground (Lillesand et al., 2004), varied for the 'glaciolacustrine', 'fluvial', and 'till' classes, but was consistently lowest in the 'bedrock' class. This is a result of the variability within the 'bedrock' class. The kappa coefficient values indicate relatively good agreement between the classified maps and training areas. When comparing the maps and the training areas, group A provided slightly better results than group B.(Table 10 and 11).

**Table 10.** Accuracy assessment of the classified map derived from group A training areas (Fig. 10a).

| Classified (predictive) map | Accuracy/ Kappa coefficient | |
|---|---|---|
| | Unfiltered | Filtered |
| Derived from Group A training areas | 90.8%/0.83 | 92.3%/0.86 |
| Derived from Group B training areas | 78.9%/0.64 | 80.9%/0.66 |

**Table 11.** Accuracy assessment of the classified map derived from group B training areas (Fig. 10b).

| Classified (predictive) map | Accuracy/ Kappa coefficient | |
|---|---|---|
| | Unfiltered | Filtered |
| Derived from Group A training areas | 85.9%/0.76 | 84.6%/0.73 |
| Derived from Group B training areas | 82.0%/0.68 | 89.5%/0.81 |

**Table 12**. Accuracy of the unfiltered classified map from group A training areas compared with point data collected in the field. The average accuracy is 49.75%.

| Group A | Fluvial | Bedrock | Glaciolacustrine | Till |
|---|---|---|---|---|
| Fluvial | 25.00 | 1.03 | 33.33 | 6.85 |
| Bedrock | 25.00 | 47.42 | 0.00 | 24.66 |
| Glaciolacustrine | 8.33 | 0.00 | 19.05 | 2.74 |
| Till | 41.67 | 51.55 | 47.62 | 65.75 |

**Table 13.** Accuracy of the filtered classified map from group A training areas compared with point data collected in the field. The average accuracy is 49.75%.

| Group A | Fluvial | Bedrock | Glaciolacustrine | Till |
|---|---|---|---|---|
| Fluvial | 41.67 | 0.00 | 33.33 | 6.85 |
| Bedrock | 16.67 | 51.58 | 0.00 | 31.51 |
| Glaciolacustrine | 8.33 | 0.00 | 14.29 | 2.74 |
| Till | 33.33 | 48.42 | 52.38 | 58.90 |

**Table 14.** Accuracy of the unfiltered classified map from group B training areas compared with point data collected in the field. The average accuracy is 50.24%.

| Group A | Fluvial | Bedrock | Glaciolacustrine | Till |
|---|---|---|---|---|
| Fluvial | 25.00 | 6.19 | 28.57 | 4.11 |
| Bedrock | 33.33 | 49.48 | 0.00 | 27.40 |
| Glaciolacustrine | 0.00 | 0.00 | 23.81 | 5.48 |
| Till | 41.67 | 44.33 | 47.62 | 63.01 |

**Table 15**. Accuracy of the filtered map from group B training areas compared with point data collected in the field. The average accuracy is 50.49%.

| Group A | Fluvial | Bedrock | Glaciolacustrine | Till |
|---|---|---|---|---|
| Fluvial | 16.67 | 5.21 | 33.33 | 5.48 |
| Bedrock | 25.00 | 54.17 | 0.00 | 30.14 |
| Glaciolacustrine | 8.33 | 0.00 | 19.05 | 4.11 |
| Till | 50.00 | 40.63 | 47.62 | 60.27 |

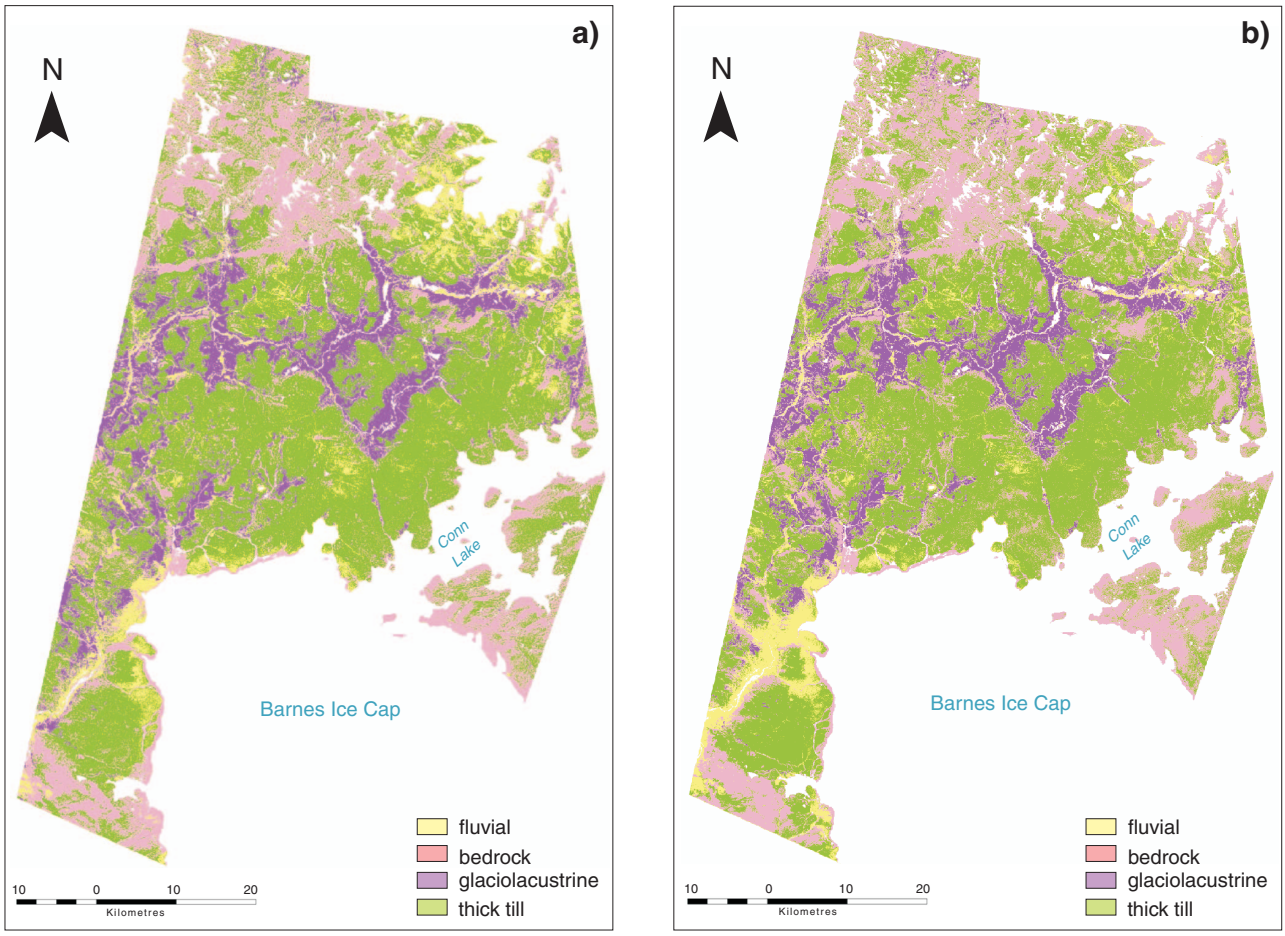


**Figure 11.** Classification maps created using all training sites with **a)** Landsat data only and **b)** Landsat TM and DEM data.

However, group A and B training areas produced nearly the same overall level of accuracy, approximately 50%, when compared with point data collected in the field (Tables 12, 13, 14 and 15). Post-classification filtering of the maps marginally improved the classification results.

## Complete classification

Classifications were run on the Landsat TM data and on the combined Landsat TM and DEM data using all training areas (Fig. 11). The average accuracy for the classification based on the Landsat data using all training areas was 85%, with a kappa coefficient of 0.74 when compared with the training areas. Combining the Landsat and DEM data improved results by only 1%; the kappa coefficient remained the same. The accuracy results for the two classifications, when compared with the field point data, were the same, i.e. 49%. As with the divided training groups, the greatest confusion was between the 'bedrock' and 'till' classes.

A cross-correlation between the two classified maps (Landsat TM only and combined Landsat TM and DEM) indicated that they are almost identical (95% agreement between the maps). For this map-to-map comparison (cross-correlation), the greatest difference was between the 'fluvial' classes where only 7% of pixels were in agreement.

Exclusion errors (excluding an area from a given surficial class when it truly belongs to that class) and commission errors (including an area in a given surficial class when it does not belong to that class) were greatest for the 'fluvial' class, indicating that the most number of fluvial pixels were incorrectly classified. The lowest exclusion and commission errors were for the 'till' class, indicating that the greatest number of till pixels were correctly classified.

# DISCUSSION

The importance of selecting representative training areas is highlighted in this study as 5 to 10% variability in the accuracy of the classified maps resulted when using different training groups. However, even with the apparent prudent selection of training areas, difficulties can still arise when trying to define training areas for surficial classes from either ground-based observations or high-resolution airphotos and

then applying these to imagery such as Landsat, which is characterized by moderate spatial resolutions (i.e. 30 m). What Landsat "sees" from a spectral point of view can be quite different from what is seen on the ground or in high-resolution imagery. High-resolution imagery captures more surface textural and contextual spatial variations as seen by an observer on the ground as well as what is captured on airphotos. Lower resolution imagery averages out these textural variations. This study has based classification on just the spectral properties of Landsat data; future studies will incorporate textural measures in an attempt to capture more of the detailed information seen on the ground or in higher resolution remotely sensed data.

Accuracy results when compared with the training areas were generally good (~80–90%). However, when compared with the field observations on surficial materials, the accuracy of the maps was much lower (~50%). This does not meet the stated goal of predicting till with 80% accuracy. This is not an unexpected result given the discrepancy between scale (resolution) of training area definition and the data used for classification. This is in part due to what the observer "sees" on the ground and the data he uses to define the training areas and the data to which the classification is applied. Areas of thin till and bedrock can be difficult to separate even in the field given the transitional and heterogeneous nature of the two material types. Given the lower resolution of the Landsat data, this problem is compounded when attempting to undertake classification using only a spectral signature. Furthermore, Landsat is unable to "capture" smaller areas of outcrop given its 30 m resolution limitation. However, from a mapping perspective, being 50% correct may be better than going out in the field with no information at all!

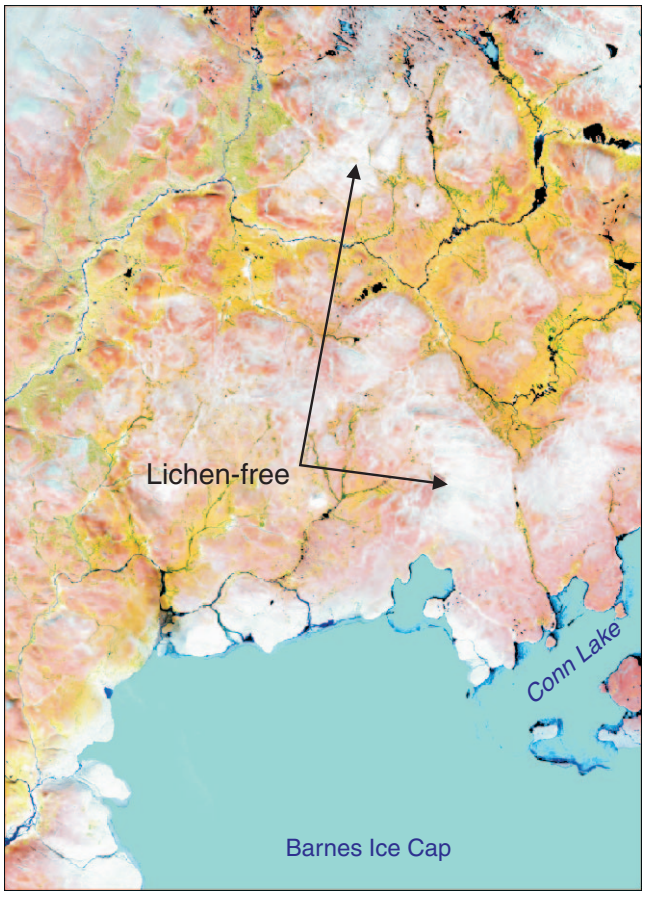


**Figure 12**. Landsat TM 5, 4, 3 false-colour composite showing lichen-free areas.

Post-classification filtering is recommended as classification accuracies improved when comparing the filtered maps and the training areas. The incorporation of topographic information (DEM) is also recommended as the statistical separation between training areas improved when the DEM was incorporated into the Landsat data in the classification process. Furthermore, classification accuracies improved slightly.

With respect to the visual appearance of surficial units on the Landsat imagery of the study area, lichen-free areas, which commonly occur at higher elevations, appeared very bright compared to surrounding areas (Fig. 12). Fluvial materials also appeared bright on the imagery but did not occur at high elevation. Prior to incorporating the DEM data into the classification, lichen-free areas were confused with fluvial material. An attempt to classify lichen-free areas separately was made to improve classification results, but was unsuccessful. The most heavily vegetated areas commonly corresponded to areas of glaciolacustrine cover. For this reason, masking vegetation did not substantially improve results.

## FUTURE STUDIES

RADARSAT data are available for this study area. To assist in distinguishing the surficial units, RADARSAT data will be added to the data set in future studies. Radar data can provide a different perspective on the surficial geology of the area given that radar is sensitive to surface roughness and moisture variations. Both of these parameters are useful for classifying the morphological and textural properties of various surficial units (Grunsky et al., 2006). In addition to capturing textural variations using radar data or textural measures derived from Landsat data (co-occurrence matrices), classifications will be tested on raw data and derivative images (i.e. ratios) using maximum likelihood and other classification algorithms (i.e. neural networks). In addition, to further evaluate the usefulness of predictive maps derived from remotely sensed data, a comparison of the classified maps and the 1:100 000 scale surficial geology maps produced by traditional field mapping approaches will be undertaken.

## ACKNOWLEDGMENTS

The authors would like to thank Don James and Danny Wright from the Geological Survey of Canada for thorough reviews of this paper that have greatly improved the content and presentation.

## REFERENCES

**Bostock, H.S.**
1970: Physiographic regions of Canada; Geological Survey of Canada, Map 1254, scale 1:500 000.

**Cohen, J.**
1960: A coefficient of agreement for nominal scales; Educational and Psychological Measurement, v. 20, p. 37–46.

**Grunsky, E., Harris, J.R., and McMartin, I.**
2006: Predictive mapping of surficial material, Schultz Lake (NTS 66A), Nunavut, Canada; Geological Survey of Canada, Open File 5153, 49 p.

**Harris, J.R., Rencz, A.N., Ballantyne, B., and Sheridon, C.**
1998: Mapping altered rocks using Landsat TM and lithogeochemical data: Sulphurets-Brucejack Lake district, British Columbia, Canada; Journal of Photogrammetric Engineering and Remote Sensing, v. 64, no. 4, p. 309–322.

**Hodgson, D.A. and Haselton, G.M.**
1974: Reconnaissance glacial geology, northeastern Baffin Island; Geological Survey of Canada, Paper 74-20, 10 p.

**Jackson, G.D.**
2000: Geology of the Clyde-Cockburn land map area, north-central Baffin Island, Nunavut; Geological Survey of Canada, Memoir 440, 303 p.

**Jensen, J.R.**
1995: Introductory Digital Image Processing: A Remote Sensing Perspective, 2nd edition; Prentice Hall, 316 p.

**Lillesand T.M., Kieffer, R.W., and Chipman, J.W.**
2004: Remote Sensing and Image Interpretation, 5th edition; John Wiley & Sons Inc., New York.

**Little, E.C., Holme, P.J., Hilchey, A.C., and Young, M.D.**
2004: Glacial geology, ice-movement chronology, and drift prospecting in the vicinity of Icebound Lakes, northern Baffin Island, Nunavut; Geological Survey of Canada, Current Research 2004-B1, 16 p.

**Ranson, K.J., Kovacs, K., Sun, G., and Kharuk, V.I.**
2003: Disturbance recognition in boreal forest using radar and LANDSAT-7; Canadian Journal of Remote Sensing, v. 29, no. 2, p. 271–285.

**Rencz, A., Harris, J., Sangster, D., and Budkewitsch, P.**
2000: Spectral characteristics of bedrock map units using LANDSAT TM and topographic data: application to bedrock mapping in Borden Peninsula, Nunavut; Geological Survey of Canada, Current Research 2000-C4, 7 p.

**Richards, J.A. and Jia, X.**
2006: Remote Sensing Digital Image Analysis: An Introduction, 4th edition; Springer-Verlag, New York, 439 p.

**Utting, D., Little, E., Coulthard, R.D., Brown, O.H., Hartman, G.M.D., Huscroft, C.A., and Smith, J.S.**
2006: Glacial history and drift prospecting, Conn Lake and Buchan Gulf, northern Baffin Island, Nunavut; Geological Survey of Canada, Current Research 2006-C3, 11 p.

**Wolken, G.J., England, J.H., and Dyke, A.S.**
2005: Re-evaluating the relevance of vegetation trimlines in the Canadian Arctic as an indicator of Little Ice Age paleoenvironments; Arctic, v. 58, no. 4, p. 341–353.

Geological Survey of Canada Project Y03